Effect of a Spatially Distributed Reaction Zone on Regular and Mach Reflection of a Detonation

Mark Short, Carlos Chiquete and Stephen Voelkel
Shock and Detonation Physics, Los Alamos National Laboratory,
Los Alamos, NM 87544, USA

1 Introduction

The flow patterns generated by an inert shock reflected from a rigid boundary have been extensively studied, and can consist of regular, Mach and von Neumann structures [1]. Similarly, a number of studies have been conducted on reflection patterns for gaseous detonations [2,3]. Significantly less is known about the reflection of detonations in condensed-phase explosives at a confining surface. In a recent study, Bdzil and Short [4] examined the flow structures that can develop when a small-resolved heat release (SRHR) condensed-phase detonation wave obliquely impacts a rigid wall at small incident angles. In simulations of condensed-phase detonation propagation in a confined two-dimensional circular arc geometry, Short et al. [5] have shown that a series of regular or Mach reflection structures can result as a consequence of the detonation impacting the outer surface of the arc. One feature that detonations in both gaseous and condensed-phase explosives have in common is that the energy release associated with a finite reaction rate has the ability to turn flow streamlines. In turn, this can affect significantly the flow structures determining the detonation wave reflection patterns.

Two models are commonly used to describe detonation propagation in condensed-phase explosives. Since the scale of the reaction zone is often significantly less than the characteristic geometry scale, one model assumes that the energy release associated with reaction is instantaneous, so that the "shock" jump incorporates the reaction energy release. This is commonly known as the Chapman-Jouguet (CJ) detonation model. The second assumes that the reaction zone is fully distributed spatially. In reality, detonations in many carbon-rich explosives consist a region of very rapid reaction, followed by region of significantly slower reaction [4], and so incorporate features of both models in their dynamic flow behavior. In the following work, we examine the flow reflection patterns and streamline turning ability of a detonation traveling at the CJ speed impacting a rigid wall wherein a certain specified amount of the energy due to reaction is released instantaneously, with the remaining released over a finite length scale. At its two limits, we recover both the CJ detonation and fully distributed reaction models.

2 Model

We model the flow in the explosive with the compressible Euler equations,

$$\frac{D\rho}{Dt} + \rho\nabla\cdot\mathbf{u} = 0, \quad \frac{D\mathbf{u}}{Dt} = -\frac{1}{\rho}\nabla p, \quad \frac{De}{Dt} = \frac{p}{\rho^2}\frac{D\rho}{Dt}, \tag{1}$$

Correspondence to: short1@lanl.gov

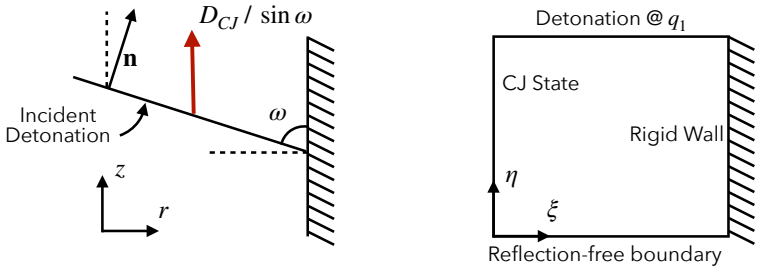

Figure 1: (Left) Schematic of a detonation traveling with $D_n = D_{CJ}$ impacting obliquely on a rigid wall at an angle ω. At $t = 0$, the detonation is traveling relative to the wall the wall at speed $D_{CJ}/\sin\omega$. (Right) The shock-fit frame used for the computations.

for density ρ, pressure p, particle velocity $\mathbf{u} = (u, v)$ and specific internal energy e. The material derivative is given by $D/Dt = \partial/\partial t + \mathbf{u}\cdot\nabla$, where t is time. We employ an idealized condensed-phase detonation model [5, 6], wherein the equation of state (EOS) model for the internal energy, e, and the frozen sound speed, c, are given by

$$e = \frac{p + A}{(\gamma - 1)\rho} - q, \quad c = \left[\frac{\gamma p + A}{\rho}\right]^{1/2}, \tag{2}$$

respectively, where γ is the adiabatic exponent and A is the stiffened gas constant. Reaction occurs through a sequential two-stage process, where the specific reaction enthalpy q is given by

$$q = q_1\lambda_1 + q_2\lambda_2, \tag{3}$$

where λ_1 and λ_2 are the reaction progress variables for the first and second reaction stages, respectively, with $0 \le \lambda_{1,2} \le 1$. For this model, the rate of the first reaction stage is assumed to be instantaneous, while that associated with the second stage is given by

$$\frac{D\lambda_2}{Dt} = kp^n(1 - \lambda_2)^\nu, \tag{4}$$

where k is a rate constant, n is the pressure exponent and ν is a reaction order variable. From the steady flow relations associated with (1), we obtain the following relation between the reaction enthalpy and the CJ speed:

$$q_1 + q_2 = \frac{D_{CJ}^2}{2(\gamma^2 - 1)}\left(1 - \frac{A}{\rho_0 D_{CJ}^2}\right)^2, \tag{5}$$

where ρ_0 is the initial density of the HE and D_{CJ} is the CJ speed.

We now define $\epsilon \in [0, 1]$ as the fraction of the overall specific reaction enthalpy contribution due to the second-stage reaction, so that

$$\frac{q_2}{q_1 + q_2} = \epsilon, \quad q_1 = \frac{D_{CJ}^2}{2(\gamma^2 - 1)}\left(1 - \frac{A}{\rho_0 D_{CJ}^2}\right)^2(1 - \epsilon), \quad q_2 = \frac{\epsilon D_{CJ}^2}{2(\gamma^2 - 1)}\left(1 - \frac{A}{\rho_0 D_{CJ}^2}\right)^2. \tag{6}$$

When $\epsilon = 0$, then $q_2 = 0$ and we recover the detonation model consisting of an instantaneous reaction. When $\epsilon = 1$, then $q_1 = 0$ and we recover the detonation model consisting of a detonation shock and fully spatially-distributed reaction zone. Reference scales are given in [5], where now the reference length scale is the length in the steady, planar Chapman-Jouguet detonation wave where $\lambda_2 = 0.5$. We take

$$\rho_0 = 2,\ A = 12.8,\ D_{CJ} = 8,\ \gamma = 3,\ n = 1,\ \nu = 1/2, \tag{7}$$

as with previous studies [5, 6], for which $q_1 + q_2 = 3.24$. The rate constant k is determined by setting the above reference length scale.

For any given detonation speed normal to the front, D_n, we can define the jump conditions behind the first instantaneous reaction stage as,

$$\rho = (\gamma+1)\rho_0 \left[\gamma + \frac{A}{\rho_0 D_{CJ}^2}\left(\frac{D_{CJ}^2}{D_n^2}\right) - \xi\right]^{-1}, \quad u_n^l = \frac{D_n}{\gamma+1}\left[1 + \xi - \frac{A}{\rho_0 D_{CJ}^2}\left(\frac{D_{CJ}^2}{D_n^2}\right)\right], \\ p = \frac{\rho_0 D_n^2}{\gamma+1}\left[1 + \xi - \frac{A}{\rho_0 D_{CJ}^2}\left(\frac{D_{CJ}^2}{D_n^2}\right)\right], \tag{8}$$

where

$$\xi = \left[1 - \frac{D_{CJ}^2}{D_n^2}\left[1 - \frac{A^2}{\rho_0^2 D_{CJ}^4}\left(\frac{D_{CJ}^2}{D_n^2} - 1\right) - \epsilon\left(1 - \frac{A}{\rho_0 D_{CJ}^2}\right)^2\right]\right]^{1/2}. \tag{9}$$

The total energy $E = e + (u_n^l)^2/2$ at the jump is calculated from

$$E = \frac{p + A}{\rho(\gamma - 1)} - q_1 + \frac{1}{2}(u_n^l)^2. \tag{10}$$

For $\epsilon = 0$ and $D_n = D_{CJ}$, we recover the flow state for a CJ detonation model, while for $\epsilon = 1$, we recover the conditions for the jump across an inert shock with normal speed D_n. For $D_n = D_{CJ}$ and $\epsilon \in [0, 1]$,

$$\rho = (\gamma+1)\rho_0 \left[\gamma + \frac{A}{\rho_0 D_{CJ}^2} - \xi\right]^{-1}, \quad u_n^l = \frac{D_n}{\gamma+1}\left[1 + \xi - \frac{A}{\rho_0 D_{CJ}^2}\right], \tag{11}$$

$$p = \frac{\rho_0 D_n^2}{\gamma+1}\left[1 + \xi - \frac{A}{\rho_0 D_{CJ}^2}\right], \quad \xi = \sqrt{\epsilon}\left(1 - \frac{A}{\rho_0 D_{CJ}^2}\right). \tag{12}$$

3 Polar Analysis

The problem under consideration consists of a detonation traveling with $D_n = D_{CJ}$ obliquely impacting a rigid wall at an angle ω (Fig. 1) as described in [4]. We can examine how the degree of energy release at the shock due to instantaneous reaction affects the streamline turning angle θ of the flow as a function of of ω, via a shock polar analysis. This is shown schematically in Fig. 2. The flow streamline turning angle θ follows from (8), with

$$u^l = u_n^l \sin\omega, \quad v^l = u_n^l \cos\omega, \quad \tan\theta = \frac{v^l}{D_n/\sin\omega - u^l}, \tag{13}$$

where u^l and v^l are the axial and transverse flow components, respectively (Fig. 2). Figure 2(Right) shows θ as a function of ω for a range of $\epsilon \in [0, 1]$ and with $D_n = D_{CJ}$. With no instantaneous energy release ($\epsilon = 1$), the incoming streamlines are turned through a moderately large angle. As ϵ decreases and more energy is released due to instantaneous reaction, θ correspondingly decreases at any fixed ω. Consequently, increasing instantaneous energy release at the shock has the ability to progressively turn the flow back toward the incoming streamlines. For $0 < \omega < \pi/2$ and $\epsilon = 0$, where all the energy is released instantaneously, $\theta > 0$, and thus the flow is always turned anticlockwise relative the incoming streamlines. Figure 2 also shows that for a wide range of ω, the flow is supersonic behind the jump. In the case of the CJ detonation ($\epsilon = 1$) the flow behind the wave is always supersonic for $\omega < \pi/2$.

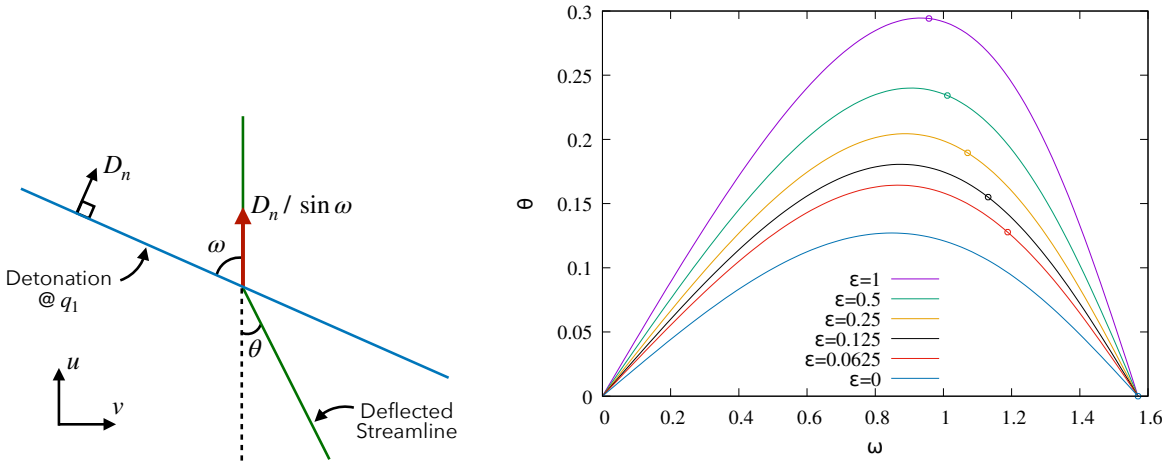

Figure 2: (Left) Schematic of shock polar construction for the streamline turning angle θ behind by an oblique wave traveling at $D_n = D_{CJ}$ with an energy release due to instantaneous reaction defined by $\epsilon \in [0, 1]$. (Right) Streamline turning angle θ as a function of ω for a range of $\epsilon \in [0, 1]$. Circles show the value of ω (ω_s) for which sonic flow occurs for each ϵ shown. Values of ω smaller than ω_s correspond to supersonic flow.

4 Numerical Computation - Shock Attached Frame

The flow equations (1) are mapped to a shock-fit frame drawn schematically in Fig. 1. The standard integration methodology follows that in [7], and typically involves needing to calculate the shock acceleration $\partial D_n/\partial\tau$, where τ is the transformed time variable. Then,

$$\frac{\partial D_n}{\partial \tau} = \left(\frac{\partial(|J|_s \rho E)}{\partial \tau} - \rho E \frac{\partial |J|_s}{\partial \tau} \right) \Bigg/ \left(|J|_s \frac{\partial(\rho E)}{\partial D_n} \right), \tag{14}$$

where $|J|_s$ is the determinant of the transformation Jacobian evaluated at the front. However, for a CJ detonation model ($D_n = D_{CJ}$, $\epsilon = 0$), the $\partial(\rho E)/\partial D_n$ term is singular at the sonic CJ point. Thus we make the transformation

$$\alpha = \xi + \frac{D_n}{D_{CJ}}, \quad \frac{\partial \alpha}{\partial \tau} = \left(\frac{\partial(|J|_s \rho E)}{\partial \tau} - \rho E \frac{\partial |J|_s}{\partial \tau} \right) \Bigg/ \left(|J|_s \frac{\partial(\rho E)}{\partial \alpha} \right), \tag{15}$$

where

$$\frac{\partial}{\partial \alpha}(\rho E) = \frac{1}{\gamma - 1} \frac{\partial p}{\partial \alpha} - q_1 \frac{\partial \rho}{\partial \alpha} + \frac{1}{2}(u_n^l)^2 \frac{\partial \rho}{\partial \alpha} + \rho u_n^l \frac{\partial u_n^l}{\partial \alpha}, \tag{16}$$

and

$$\frac{\partial \rho}{\partial \alpha} = \frac{\rho^2}{(\gamma + 1)\rho_0} \left[1 + \left(2 \left(\frac{A}{\rho_0 D_{CJ}^2} \right) \frac{D_{CJ}^3}{D_n^3} - 1 \right) \frac{1}{D_{CJ}} \frac{\partial D_n}{\partial \alpha} \right], \tag{17}$$

with

$$\left[\alpha - \frac{D_n}{D_{CJ}} + \frac{D_{CJ}^3}{D_n^3} \left[1 - \frac{A^2}{\rho_0^2 D_{CJ}^4} \left(2 \frac{D_{CJ}^2}{D_n^2} - 1 \right) - \epsilon \left(1 - \frac{A}{\rho_0 D_{CJ}^2} \right)^2 \right] \right] \frac{1}{D_{CJ}} \frac{\partial D_n}{\partial \alpha} = \alpha - \frac{D_n}{D_{CJ}}, \tag{18}$$

and

$$\frac{\partial u_n^l}{\partial \alpha} = \frac{\rho_0 D_n}{\rho^2} \frac{\partial \rho}{\partial \alpha} + \left(1 - \frac{\rho_0}{\rho} \right) \frac{\partial D_n}{\partial \alpha}, \quad \frac{\partial p}{\partial \alpha} = \rho_0 u_n^l \frac{\partial D_n}{\partial \alpha} + \rho_0 D_n \frac{\partial u_n^l}{\partial \alpha}. \tag{19}$$

Thereafter the flow equations are integrated with the finite volume method described in [7].

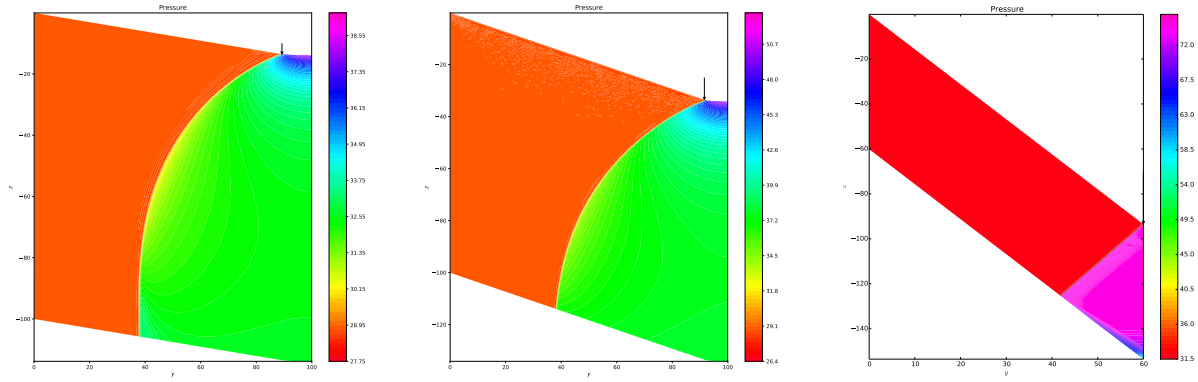

Figure 3: Pressure field wave reflection patterns for a fully instantaneous reaction zone model ($\epsilon = 0$) with $\phi = 0.15$ (left), $\phi = 0.35$ (middle) and $\phi = 0.9$ (right).

5 Regular and Mach Reflection Patterns for Partially Distributed Reaction Zones

We now conduct simulations of the impact problem for the full two-stage reaction model as desribed in §2. Figure 3 shows the wave reflection patterns for a fully instantaneous reaction zone model ($\epsilon = 0$) with impact angles $\phi = 0.15$ (left), $\phi = 0.35$ (middle) and $\phi = 0.9$, where $\phi = \pi/2 - \omega$, i.e. the initial angle of impact relative to the wall normal. Thus small ϕ corresponds to a glancing impact problem. Figure 4 shows the corresponding wave reflection patterns for a fully distributed reaction zone model ($\epsilon = 1$) with the same impact angles as Fig. 3.

For $\epsilon = 0$, the more shallow angles $\phi = 0.15$ and $\phi = 0.35$ exhibit a Mach reflection pattern, in which the reflected shock attaches to the instantaneous detonation front. For the larger angle $\phi = 0.9$, a reflected shock wave is required to turn the flow to match the wall streamline. In contrast, the reflection patterns for a fully distributed reaction zone ($\epsilon = 1$) as shown in Fig. 4 are substantially different from those observed in Fig. 3 for the same impact angles. For $\phi = 0.15$, we observe a continuous reaction zone structure with no discontinuous reflected wave present. The flow downstream of the reaction zone also remains smooth. This indicates that exothermic energy release in a spatially distributed reaction zone has the ability to turn the flow streamlines to satisfy the boundary conditions established by the rigid wall. For $\phi = 0.35$, we again observe a continuous reaction zone structure, with no discontinuous reflected wave present. However, downstream of the reaction zone, compression waves steepen into a reflected shock. A forked shock structure is observed near the end of the reaction zone. For the larger angle $\phi = 0.9$, we now observe that the reflected shock has penetrated through the reaction zone and now forms a classical Mach stem structure.

In summary, exothermic energy release in a spatially distributed reaction zone plays an important role in flow streamline dynamics, and significantly affects the wave reflection patterns generated by a detonation reflected off a rigid wall. In the final paper, we will also examine the wave reflection patterns generated for $\epsilon \in (0, 1)$, i.e. for partial instantaneous energy release.

References

[1] H. Hornung. Regular and Mach reflection of shock waves. *Annu. Rev. Fluid Mech.*, 18:33–58, 1986.

[2] R.S.B. Ong. *On the interaction of a Chapman-Jouguet detonation wave with a wedge*. PhD thesis, University of Michigan, 1956.

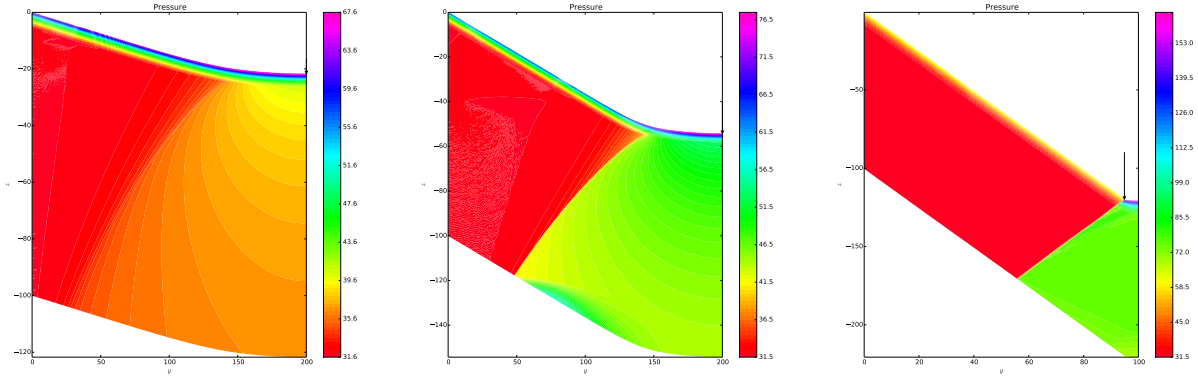

Figure 4: Pressure field wave reflection patterns for a fully distributed reaction zone model ($\epsilon = 1$) with $\phi = 0.15$ (left), $\phi = 0.35$ (middle) and $\phi = 0.9$ (right).

[3] J.E. Shepherd, E. Schultz, and R. Akbar. Detonation diffraction. In G.J. Ball, R. Hillier, and G.T. Roberts, editors, *Proc. 22nd Int. Symp. on Shock Waves*, pages 41–48, 1999.

[4] J.B. Bdzil and M. Short. Theory of Mach reflection of detonation at glancing incidence. *J. Fluid Mech.*, 811:269–314, 2017.

[5] M. Short, J.J. Quirk, C.D. Chiquete, and C.D. Meyer. Detonation propagation in a circular arc: Reactive burn modelling. *J. Fluid Mech.*, 835:970–998, 2018.

[6] M. Short and J.J. Quirk. High explosive detonation-confiner interations. *Annu. Rev. Fluid Mech.*, 50:215–242, 2018.

[7] C. Chiquete, M. Short, C.D. Meyer, and J.J. Quirk. Calibration of the pseudo-reaction-zone model for detonation wave propagation. *Combust. Theory Modell.*, 22:744–766, 2018.